

MANIFOLDS OF EQUILIBRIA AND BIFURCATIONS WITHOUT PARAMETERS IN MEMRISTIVE CIRCUITS*

RICARDO RIAZA†

Abstract. The memory-resistor or *memristor* is a new electrical device governed by a nonlinear flux-charge relation. Its existence was predicted by Leon Chua in 1971, and the report in 2008 of a physical device with such a constitutive relation has driven a lot of attention to this circuit element. The memristor and related devices are expected to play a very relevant role in electronics in the near future, specially at the nanometer scale. The special form of the voltage-current characteristic, which reads as either $v = M(q)i$ or $i = W(\varphi)v$, implies that any equilibrium point is embedded into a center manifold of equilibria whose dimension is defined by the total number of memristors in the circuit. We characterize the normal hyperbolicity of these manifolds of equilibria in graph-theoretic terms. Moreover, when the assumptions supporting the normal hyperbolicity of such manifolds fail, the differential-algebraic nature of circuit models is shown to lead to certain bifurcations without parameters not exhibited by explicit ODEs. The results are illustrated by several circuit examples, some of which arise in the design of superconducting quantum bits based on the Josephson junction.

Key words. manifold of equilibria, normal hyperbolicity, differential-algebraic equation, bifurcation without parameters, nonlinear circuit, memristor, qubit, Josephson junction

AMS subject classifications. 34A09, 34C45, 34D35, 37G10, 94C05, 94C15

DOI. 10.1137/100816559

1. Introduction. Research on the dynamics near manifolds of nonisolated equilibria has been motivated by theoretical reasons and also by the appearance of such manifolds in a variety of applications [2, 3, 15, 16, 17, 18]. As reported in these references, such applications arise, e.g., in population genetics, game theory, or in the analysis of networks of coupled oscillators and systems of hyperbolic conservation laws. In a C^1 continuous-time setting, and provided that the manifold of equilibria is m -dimensional, then at least m eigenvalues of the linearization about any of these equilibria do vanish; the manifold is said to be *normally hyperbolic* if the remaining eigenvalues are away from the imaginary axis. At points of the manifold where the normal hyperbolicity requirement fails the qualitative properties of equilibria change, and a *bifurcation without parameters* is said to occur (cf. [15, 16, 17]).

In the present paper we discuss this type of phenomenon in the context of memristive circuits. The memristor (or memory-resistor) is a novel electrical device characterized by a nonlinear C^1 characteristic $\varphi = \phi(q)$ relating the flux and the charge; this yields a voltage-current relation of the form $v = M(q)i$, where $M(q) = \phi'(q)$ is the *memristance*. The name comes from the fact that in this voltage-current constitutive relation, the memristance $M(q) = M(\int_{-\infty}^t i(\tau)d\tau)$ keeps track of the device history. In a flux-controlled context, the characteristic reads as $q = \sigma(\varphi)$; now the current-voltage relation is $i = W(\varphi)v$, where $W(\varphi) = \sigma'(\varphi)$ is the so-called *memductance* and depends on $\int_{-\infty}^t v(\tau)d\tau$.

Two milestones in the literature on memristors are Chua's seminal work [8] and

*Received by the editors December 1, 2010; accepted for publication (in revised form) March 12, 2012; published electronically June 21, 2012. This work was supported by Research Projects MTM2010-15102 of Ministerio de Ciencia e Innovación and CCG10-UPM/ESP-5236 of Comunidad de Madrid/UPM, Spain.

<http://www.siam.org/journals/siap/72-3/81655.html>

†Dept. Matemática Aplicada a las Tecnologías de la Información, ETSI Telecomunicación, Universidad Politécnica de Madrid, Ciudad Universitaria s/n - 28040 Madrid, Spain (ricardo.riaza@upm.es).

the paper [43] by Strukov et al. The memristor was postulated by Chua in 1971 to be the fourth basic circuit element for symmetry reasons, since resistors, capacitors, and inductors are defined by voltage-current, charge-voltage, and flux-current relations, respectively, and a charge-flux characteristic was somehow lacking [8]. The appearance of the device at the nanometer scale in 2008, as reported in [43], has driven a lot of attention to the memristor; much research is focused on its analytical properties [4, 21, 23, 26, 27, 28, 39, 42], and many applications of these and other related devices are being reported [12, 22, 24, 26, 31, 32, 33]. Commercial memory chips based on the memristor are planned to be released in 2013 [1].

If ϕ in the characteristic above were linear (making M actually independent of q), the constitutive relation of a memristor would make no difference to that of a linear resistor. Therefore, the characteristic ϕ is intrinsically nonlinear. From a local point of view, the form of the memristor constitutive relation will be responsible for the existence of a center manifold of equilibria, as detailed later. These manifolds of equilibria have been already observed in specific circuit examples (cf. [26, 39]). In the present paper we tackle the normal hyperbolicity of such manifolds in general memristive circuits, discussing circuit-theoretic conditions under which this normal hyperbolicity holds and addressing certain related stability properties.

Our goal is to perform this analysis in terms of the topological (graph-theoretic) properties of the circuit, the approach being based on the use of semistate models formulated in terms of differential-algebraic equations (DAEs) [14, 19, 35, 37, 40, 41, 44, 45]. These models are presented in section 2. The main results of the paper are discussed in section 3, where we address in graph-theoretic terms the normal hyperbolicity of manifolds of equilibria arising in memristive circuits. Cases in which the conditions supporting normal hyperbolicity fail motivate the analysis of certain bifurcations without parameters in semiexplicit DAEs, carried out in section 4; specifically, a phenomenon of eigenvalue divergence (sometimes referred to as a *singularity-induced bifurcation* [5, 38, 46, 47]), which derives from the differential-algebraic nature of nonlinear circuit models, will be characterized here for the first time in a context without parameters. Our results will be illustrated in section 5 by several circuit examples; some of them arise in the design of *quantum bits* or *qubits*, a basic element in quantum computation [10, 29, 32]. The implementation of qubits is often based on the Josephson tunneling junction, accurate models of which involve a flux-controlled memristor. Finally, some concluding remarks are compiled in section 6.

2. Memristive circuits, DAE models, and equilibria.

2.1. Nonlinear circuits with memristors. We will analyze the dynamical behavior near manifolds of equilibria of connected, time-invariant, nonlinear circuits including capacitors, inductors, memristors, resistors, and voltage and current sources. The working assumptions on the different devices are compiled in this section.

Nonlinear capacitors may in general be either charge-controlled or voltage-controlled. In a charge-controlled context, the characteristic of capacitors reads as $v_c = \xi(q_c)$, and the corresponding circuit model involves the capacitor charges. For the sake of simplicity, capacitors will be assumed to be governed by a voltage-controlled characteristic $q_c = \psi(v_c)$, with incremental capacitance matrix $C(v_c) = \psi'(v_c)$. Throughout the paper all maps are assumed to be sufficiently differentiable. Analogously, nonlinear inductors may be defined either by a flux-controlled relation $i_l = \chi(\varphi_l)$ or by a current-controlled one $\varphi_l = \eta(i_l)$; we will assume the latter case in this and the next section, denoting by $L(i_l)$ the incremental inductance matrix $\eta'(i_l)$. The results can be extended without difficulty to problems with charge-controlled capacitors and/or flux-

controlled inductors; actually, the circuits involving Josephson junctions in section 5 will illustrate how flux-controlled inductors can be handled in the same manner.

Memristors will be assumed to be flux-controlled; that is, they will be governed by a characteristic of the form $q_m = \sigma(\varphi_m)$; the memductance matrix will be $W(\varphi_m) = \sigma'(\varphi_m)$. In turn, resistors will be assumed to be voltage-controlled by a map of the form $i_r = \gamma(v_r)$, and we let $G(v_r)$ stand for the incremental conductance matrix $\gamma'(v_r)$. Again, the control assumptions on memristors and resistors are meant for simplicity, but the results hold for circuits including also charge-controlled memristors and/or current-controlled resistors. Note that the nonlinear nature of these characteristics allows us to consider, for instance, a diode as a nonlinear resistor. Also for the sake of simplicity, voltage and current sources will be assumed to be independent; their excitation terms will be written as $v_s(t)$ and $i_s(t)$, respectively.

In certain parts of our analysis we will assume that capacitors, inductors, memristors, and/or resistors are strictly locally passive; this means that the matrices $C(v_c)$, $L(i_l)$, $W(\varphi_m)$, and $G(v_r)$ are positive definite. Recall that a square matrix P is positive definite if it verifies $v^T P v > 0$ for all nonvanishing real vectors v . We do not require P to be symmetric. Coupling effects are allowed within each one of these sets of devices, so that the corresponding matrices need not be diagonal.

Under these assumptions, the circuit equations can be written in the differential-algebraic form

$$\begin{aligned}
 (1a) \quad & C(v_c)v'_c = i_c, \\
 (1b) \quad & L(i_l)i'_l = v_l, \\
 (1c) \quad & \varphi'_m = v_m, \\
 (1d) \quad & 0 = i_m - W(\varphi_m)v_m, \\
 (1e) \quad & 0 = i_r - \gamma(v_r), \\
 (1f) \quad & 0 = B_c v_c + B_l v_l + B_m v_m + B_r v_r + B_v v_s(t) + B_i v_i, \\
 (1g) \quad & 0 = Q_c i_c + Q_l i_l + Q_m i_m + Q_r i_r + Q_v i_v + Q_i i_s(t).
 \end{aligned}$$

We are expressing Kirchhoff laws in terms of the loop and cutset matrices as $Bv = 0$, $Qi = 0$, respectively (cf. subsection 3.2 below). The loop matrix B is split as $(B_c \ B_l \ B_m \ B_r \ B_v \ B_i)$, where B_c (resp., B_l , B_m , B_r , B_v , B_i) corresponds to the columns accommodating capacitors (resp., inductors, memristors, resistors, voltage sources, current sources). The same applies to the cutset matrix Q .

2.2. Differential-algebraic circuit models and equilibria. Assume that the voltage and current sources are DC ones, so that $v_s(t)$ and $i_s(t)$ in (1f)–(1g) take on fixed, constant values V , I . The circuit model (1) then has the form of an autonomous DAE, namely,

$$\begin{aligned}
 (2a) \quad & E(x)x' = f(x, y), \\
 (2b) \quad & 0 = g(x, y),
 \end{aligned}$$

where x and y stand for the variables (v_c, i_l, φ_m) and $(i_c, v_l, v_m, i_m, v_r, i_r, v_i, i_v)$. The maps f and g capture the right-hand sides of (1a)–(1c) and (1d)–(1g), respectively, whereas $E(x)$ is the block-diagonal matrix block-diag($C(v_c)$, $L(i_l)$, I_m). The incremental capacitance and inductance matrices will be nonsingular throughout the paper, making $E(x)$ itself nonsingular.

Under certain assumptions to be detailed later, the matrix of partial derivatives g_y will be nonsingular around a given (x^*, y^*) satisfying (2b). This gives the DAE

(2) an *index one* structure [7, 34, 37]. When this is the case, (2b) can be locally described as $y = h(x)$ for a certain map h , as an easy consequence of the implicit function theorem, and the DAE admits the local reduction

$$(3) \quad E(x)x' = f(x, h(x)).$$

For the sake of simplicity our attention will be mostly restricted to an index one setting, although the results can be extended to index two configurations (cf. Remark 1 in section 3.3 and also Example 2 in section 5).

Equilibria (x^*, y^*) of (2) are defined by the conditions $f(x^*, y^*) = g(x^*, y^*) = 0$. In turn, the Jacobian matrix of $F(x) = E^{-1}(x)f(x, h(x))$ at x^* (which is an equilibrium of (3)) is

$$(4) \quad J = E^{-1}(x^*)(f_x - f_y g_y^{-1} g_x)|_{(x^*, h(x^*))}.$$

The key properties of the local dynamics of (1) near an equilibrium state will be defined by the eigenvalues of (4), as detailed in what follows.

3. Normally hyperbolic manifolds of equilibria.

3.1. Manifolds of equilibria in circuits with memristors. Equilibrium points of (1) are defined by the conditions

$$(5a) \quad i_c = v_l = 0, \quad v_m = i_m = 0, \quad i_r = \gamma(v_r),$$

$$(5b) \quad 0 = B_c v_c + B_r v_r + B_v V + B_i v_i,$$

$$(5c) \quad 0 = Q_l i_l + Q_r i_r + Q_v i_v + Q_i I.$$

Note that the memristors' fluxes φ_m are not at all involved in these equations; this means that any equilibrium point belongs to a manifold of equilibria whose dimension equals the number of memristors. This holds also in the presence of charge-controlled memristors, since in that case the memristor charges do not enter the equilibrium conditions, either.

Obviously, in this situation the linearization about any of these equilibria displays at least m zero eigenvalues (i.e., the algebraic multiplicity of the zero eigenvalue is greater than or equal to m), where m stands for the number of memristors. Our goal is to provide conditions under which the remaining eigenvalues are neither zero (that is, the algebraic multiplicity of the zero eigenvalue actually equals m) nor purely imaginary, thereby guaranteeing the normal hyperbolicity of such manifolds.

3.2. Auxiliary notions and results from digraph theory. Our analysis makes systematic use of several concepts coming from digraph theory, compiled below. The reader is referred to [6, 13, 37] for more detailed discussions of these notions.

Digraph matrices. The statement of Kirchhoff laws in the form depicted in (1f)–(1g) is based on the use of reduced loop and cutset matrices. Choosing an orientation in every loop (or *cycle*), the *loop matrix* \tilde{B} is defined as (b_{ij}) , where

$$b_{ij} = \begin{cases} 1 & \text{if branch } j \text{ is in loop } i \text{ with the same orientation,} \\ -1 & \text{if branch } j \text{ is in loop } i \text{ with the opposite orientation,} \\ 0 & \text{if branch } j \text{ is not in loop } i. \end{cases}$$

The rank of this matrix can be shown to equal $e - n + k$, where e , n , and k are the numbers of branches, nodes, and connected components, respectively. A *reduced loop matrix* B is any $((e - n + k) \times e)$ -submatrix of \tilde{B} with full row rank.

In turn, a subset K of the set of branches of a digraph is a *cutset* if the removal of K increases the number of connected components of the digraph, and it is minimal with respect to this property; that is, the removal of any proper subset of K does not increase the number of components. The removal of the branches of a cutset increases the number of connected components by exactly one. Furthermore, all the branches of a cutset may be shown to connect the same pair of connected components of the digraph which results from the deletion of the cutset. This makes it possible to define the orientation of a cutset, say from one of these components towards the other. The cutset matrix $\tilde{Q} = (q_{ij})$ is then defined by

$$q_{ij} = \begin{cases} 1 & \text{if branch } j \text{ is in cutset } i \text{ with the same orientation,} \\ -1 & \text{if branch } j \text{ is in cutset } i \text{ with the opposite orientation,} \\ 0 & \text{if branch } j \text{ is not in cutset } i. \end{cases}$$

The rank of \tilde{Q} can be proved to be $n - k$; any set of $n - k$ linearly independent rows of \tilde{Q} defines a *reduced cutset matrix* $Q \in \mathbb{R}^{(n-k) \times e}$.

Cycle and cut spaces. Loops and cutsets can be associated in a natural way with vectors in \mathbb{R}^e , their entries (b_1, \dots, b_e) , (q_1, \dots, q_e) being just given by fixing i in the definitions of b_{ij} and q_{ij} above. The *cycle* and *cut* spaces \mathcal{B} , \mathcal{Q} are the linear subspaces of \mathbb{R}^e spanned by these vectors. They have dimensions $e - n + k$ and $n - k$, and bases for them are defined by the rows of any reduced loop or cutset matrices, respectively. This means that the cycle space \mathcal{B} equals $\text{im } B^T$ and, analogously, that the cut space \mathcal{Q} is defined by $\text{im } Q^T$. The cut space \mathcal{Q} can be also described as $\text{im } A^T$, in terms of a *reduced incidence matrix* A (cf. [37]).

Moreover, these two spaces are orthogonal to each other (see, e.g., [6]). This yields the pair of relations

$$(6) \quad \mathcal{B} = \ker Q, \quad \mathcal{Q} = \ker B,$$

a description of the cycle and cut spaces which will be systematically used in later analyses. In the light of (6), Kirchhoff laws $Bv = 0$, $Qi = 0$ express that, for any solution of the circuit equations, the set of branch voltages and currents must belong to the cut and cycle spaces, respectively.

Additionally, if we restrict the attention to loops or cutsets defined by branches from within a given set K , the fact that the remaining entries in the corresponding vectors vanish makes it possible to describe the K -*cycle* and K -*cut* spaces as

$$(7) \quad \mathcal{B}_K = \ker Q_K, \quad \mathcal{Q}_K = \ker B_K,$$

in the understanding that the corresponding vectors now lie on \mathbb{R}^κ , κ being the number of branches in K . Here Q_K and B_K are the submatrices of Q and B defined by the columns whose branches belong to K . In particular, a digraph does not have K -loops or K -cutsets (i.e., loops or cutsets just defined by branches belonging to K) if and only if $\ker Q_K = \{0\}$ or $\ker B_K = \{0\}$, respectively.

3.3. Normal hyperbolicity. Our analysis will proceed in two steps: first, in Proposition 1 we show that there are no more than m null eigenvalues in the linearization about an equilibrium point, m standing for the number of memristors; after that, we prove in Proposition 2 that the linearization displays no purely imaginary eigenvalues $i\omega$ with $\omega \neq 0$. Before that we need the following auxiliary result.

LEMMA 1. *Split the branches of a given digraph into four pairwise disjoint sets K_1 , K_2 , K_3 , K_4 , and denote by B_i , Q_i the submatrices of B and Q defined by the*

columns which correspond to branches in K_i . Assume that P is a positive definite matrix and write

$$M = \begin{pmatrix} B_1 & 0 & B_3 \\ 0 & Q_2 & Q_3P \end{pmatrix}.$$

Then the identity $\ker M = \ker B_1 \times \ker Q_2 \times \{0\}$ holds. In particular, the kernel of M is trivial if and only if the digraph has neither K_1 -cutsets nor K_2 -loops.

Proof. This is an easy consequence of the fact that a vector in the kernel of M can be written as (v_1, v_2, v_3) with $B_1v_1 + B_3v_3 = 0$, $Q_2v_2 + Q_3Pv_3 = 0$. This means that $(v_1, 0, v_3, 0) \in \ker B = \mathcal{Q}$ and $(0, v_2, Pv_3, 0) \in \ker Q = \mathcal{B}$. The orthogonality of the cut and cycle spaces yields $v_3^T Pv_3 = 0$, and then $v_3 = 0$ because of the positive definiteness of P . The identities $v_1 \in \ker B_1$, $v_2 \in \ker Q_2$ follow in a straightforward manner. The last assertion is a direct consequence of (7). \square

In Proposition 1 below, a VC-loop is a loop composed only of voltage sources and/or capacitors. VL-loops, IL-cutsets, and IC-cutsets are defined analogously.

PROPOSITION 1. *Assume that a given circuit does not display VC-loops, VL-loops, IL-cutsets, or IC-cutsets. Suppose that the memductance and conductance matrices W, G are positive definite at a given equilibrium. Then the reduction (3) is locally feasible, and the linearization (4) has a zero eigenvalue whose geometric and algebraic multiplicities equal the number of memristors.*

Proof. We first need to show that the reduction (3) is feasible near the equilibrium. This will be a consequence of the fact that the matrix $g_y(x^*, y^*)$ is invertible. Indeed, this matrix reads as

$$(8) \quad g_y(x^*, y^*) = \begin{pmatrix} 0 & 0 & -W & I_m & 0 & 0 & 0 & 0 \\ 0 & 0 & 0 & 0 & -G & I_r & 0 & 0 \\ 0 & B_l & B_m & 0 & B_r & 0 & B_i & 0 \\ Q_c & 0 & 0 & Q_m & 0 & Q_r & 0 & Q_v \end{pmatrix},$$

which is nonsingular if and only if so is

$$\begin{pmatrix} 0 & B_l & B_m & B_r & B_i & 0 \\ Q_c & 0 & Q_mW & Q_rG & 0 & Q_v \end{pmatrix}.$$

By identifying K_1 -, K_2 -, and K_3 -branches with current sources and inductors, voltage sources and capacitors, and memristors and resistors, respectively, we may apply Lemma 1 in order to show that the absence of VC-loops and IL-cutsets, together with the positive definiteness of W and G , implies that $g_y(x^*, y^*)$ is nonsingular.

Now, the matrix $f_x - f_y g_y^{-1} g_x$ (evaluated at (x^*, y^*)) arising in (4) is the Schur complement [20, 37] of $g_y(x^*, y^*)$ in

$$(9) \quad H = \begin{pmatrix} H_{11} & H_{12} \\ H_{21} & H_{22} \end{pmatrix} = \begin{pmatrix} f_x & f_y \\ g_x & g_y \end{pmatrix} \Big|_{(x^*, y^*)},$$

where we are denoting

$$(10) \quad H_{11} = f_x(x^*, y^*), \quad H_{12} = f_y(x^*, y^*), \quad H_{21} = g_x(x^*, y^*), \quad H_{22} = g_y(x^*, y^*)$$

for the sake of notational simplicity. An elementary property of Schur complements states that $\text{cork}(H_{11} - H_{12}H_{22}^{-1}H_{21}) = \text{cork} H$, where the corank of a square matrix is the dimension of its kernel. Together with the fact that $E = E(x^*)$ is nonsingular, this

implies that the geometric multiplicity of the null eigenvalue of (4) can be computed as the corank of the matrix H in (9). This matrix has the form

$$(11) \quad H = \begin{pmatrix} 0 & 0 & 0 & I_c & 0 & 0 & 0 & 0 & 0 & 0 & 0 \\ 0 & 0 & 0 & 0 & I_l & 0 & 0 & 0 & 0 & 0 & 0 \\ 0 & 0 & 0 & 0 & 0 & I_m & 0 & 0 & 0 & 0 & 0 \\ 0 & 0 & 0 & 0 & 0 & -W & I_m & 0 & 0 & 0 & 0 \\ 0 & 0 & 0 & 0 & 0 & 0 & 0 & -G & I_r & 0 & 0 \\ B_c & 0 & 0 & 0 & B_l & B_m & 0 & B_r & 0 & B_i & 0 \\ 0 & Q_l & 0 & Q_c & 0 & 0 & Q_m & 0 & Q_r & 0 & Q_v \end{pmatrix}.$$

The null columns corresponding to the φ_m entries reflect that the geometric multiplicity is greater than or equal to the number of memristors. For it to actually be greater, the matrix

$$(12) \quad \begin{pmatrix} B_c & 0 & B_r & B_i & 0 \\ 0 & Q_l & Q_r G & 0 & Q_v \end{pmatrix}$$

should have a nontrivial kernel. But this is not possible because of the absence of IC-cutsets and VL-loops, together with the positive definiteness of G : indeed, this is again a consequence of Lemma 1, with K_1 -, K_2 -, K_3 -, and K_4 -branches now corresponding to current sources and capacitors, voltage sources and inductors, resistors, and memristors, respectively. The kernel of (12) is therefore trivial, and the geometric multiplicity of the zero eigenvalue indeed matches the number of memristors.

In order to show that the algebraic multiplicity of the zero eigenvalue also equals the number of memristors, we need to show that the zero eigenvalue of (4) has index one, namely, that $J^2 v = 0$ implies $Jv = 0$. From elementary linear algebra we know that this condition can be computed as $\text{im } J \cap \ker J = \{0\}$, and since $H_{11} = 0$ and E is nonsingular, this can be recast as

$$(13) \quad \text{im } E^{-1} H_{12} H_{22}^{-1} H_{21} \cap \ker H_{12} H_{22}^{-1} H_{21} = \{0\}.$$

The H_{21} matrix reads as

$$H_{21} = \begin{pmatrix} 0 & 0 & 0 \\ 0 & 0 & 0 \\ B_c & 0 & 0 \\ 0 & Q_l & 0 \end{pmatrix}.$$

As shown above, the corank of $H_{12} H_{22}^{-1} H_{21}$ equals the number of memristors, but so does the corank of the matrix H_{21} , since $\ker B_c = \{0\}$ and $\ker Q_l = \{0\}$ because of (7) and the absence of C-cutsets and L-loops, which are particular instances of IC-cutsets and VL-loops, respectively. The identity $\ker H_{12} H_{22}^{-1} H_{21} = \ker H_{21}$ follows in a straightforward manner.

Note that vectors in $\ker H_{21} = \ker H_{12} H_{22}^{-1} H_{21}$ read as $v = (0, 0, u)$, and, because of the block-diagonal form of $E = E(x^*)$, the condition $(0, 0, u) \in \text{im } E^{-1} H_{12} H_{22}^{-1} H_{21}$ amounts to requiring that $(0, 0, u) \in \text{im } H_{12} H_{22}^{-1} H_{21}$. Another property of Schur complements makes it possible to restate $v \in \text{im } H_{12} H_{22}^{-1} H_{21}$ as

$$\begin{pmatrix} v \\ 0 \end{pmatrix} \in \text{im} \begin{pmatrix} 0 & H_{12} \\ H_{21} & H_{22} \end{pmatrix},$$

that is,

$$(14) \quad \begin{pmatrix} 0 \\ 0 \\ u \\ 0 \\ 0 \\ 0 \\ 0 \end{pmatrix} = \begin{pmatrix} 0 & 0 & 0 & I_c & 0 & 0 & 0 & 0 & 0 & 0 & 0 & 0 \\ 0 & 0 & 0 & 0 & I_l & 0 & 0 & 0 & 0 & 0 & 0 & 0 \\ 0 & 0 & 0 & 0 & 0 & I_m & 0 & 0 & 0 & 0 & 0 & 0 \\ 0 & 0 & 0 & 0 & 0 & -W & I_m & 0 & 0 & 0 & 0 & 0 \\ 0 & 0 & 0 & 0 & 0 & 0 & 0 & -G & I_r & 0 & 0 & 0 \\ B_c & 0 & 0 & 0 & B_l & B_m & 0 & B_r & 0 & B_i & 0 & 0 \\ 0 & Q_l & 0 & Q_c & 0 & 0 & Q_m & 0 & Q_r & 0 & Q_v & 0 \end{pmatrix} z$$

for a certain z . Splitting the variable z , (14) easily yields

$$\begin{aligned} B_c z_1 + B_m z_6 + B_r z_8 + B_i z_{10} &= 0, \\ Q_l z_2 + Q_m W z_6 + Q_r G z_8 + Q_v z_{11} &= 0, \end{aligned}$$

so that $(z_1, 0, z_6, z_8, 0, z_{10}) \in \ker B = \mathcal{Q}$ and $(0, z_2, W z_6, G z_8, z_{11}, 0) \in \ker Q = \mathcal{B}$. Using again the orthogonality of the cut and cycle spaces, we obtain

$$z_6^T W z_6 + z_8^T G z_8 = 0,$$

and, because of the positive definiteness assumption on W and G , it follows that $z_6 = 0$ and $z_8 = 0$. The first condition is equivalent to $u = 0$, which yields $v = 0$. This means that (13) holds, showing that the zero eigenvalue has actually index one and, therefore, that the algebraic multiplicity equals as well the number of memristors, as we aimed to show. \square

The following statement extends (and simplifies the proof of) a result already known for circuits without memristors [40].

PROPOSITION 2. *Consider a circuit which exhibits neither VC-loops nor IL-cutsets. Assume that, at a given equilibrium, the memductance and conductance matrices W, G are positive definite, and the capacitance and inductance matrices C, L are symmetric and nonsingular. Either the absence of ICL-cutsets or that of VCL-loops implies that the linearization (4) has no purely imaginary eigenvalues $i\omega$ with $\omega \neq 0$.*

Proof. It is a very simple task to check that the eigenvalues of (4) or, equivalently, the eigenvalues of $\lambda E - (H_{11} - H_{12}H_{22}^{-1}H_{21})$ (with the notation of (10) and E standing for $E(x^*)$), equal those of the matrix pencil

$$(15) \quad \lambda \begin{pmatrix} E & 0 \\ 0 & 0 \end{pmatrix} - \begin{pmatrix} H_{11} & H_{12} \\ H_{21} & H_{22} \end{pmatrix}.$$

Using the form of H displayed in (11), the eigenvalue-eigenvector equations for this pencil can be easily checked to amount to the existence of $\lambda \in \mathbb{C}$ and a vector $z = (z_1, z_2, z_3, z_4, z_5, z_6)$ verifying

$$(16a) \quad B_c z_1 + \lambda B_l L z_2 + B_m z_3 + B_r z_4 + B_i z_5 = 0,$$

$$(16b) \quad \lambda Q_c C z_1 + Q_l z_2 + Q_m W z_3 + Q_r G z_4 + Q_v z_6 = 0.$$

The conjugate of (16a) reads as

$$(17) \quad B_c \bar{z}_1 + \bar{\lambda} B_l L \bar{z}_2 + B_m \bar{z}_3 + B_r \bar{z}_4 + B_i \bar{z}_5 = 0.$$

Again, the orthogonality of the cycle and cut spaces makes it possible to derive, from (16b) and (17), the relation

$$(18) \quad \lambda z_1^* C z_1 + \bar{\lambda} z_2^* L z_2 + z_3^* W z_3 + z_4^* G z_4 = 0,$$

where $*$ stands for the conjugate transpose. We have made use of the symmetry of L . Using in turn the symmetry of C , the conjugate transpose of (18) is

$$(19) \quad \bar{\lambda} z_1^* C z_1 + \lambda z_2^* L z_2 + z_3^* W^T z_3 + z_4^* G^T z_4 = 0.$$

The addition of (18) and (19) yields

$$(20) \quad 2\operatorname{Re}\lambda(z_1^* C z_1 + z_2^* L z_2) + z_3^*(W + W^T)z_3 + z_4^*(G + G^T)z_4 = 0.$$

Let us now assume that the circuit displays a (nonvanishing) purely imaginary eigenvalue $\lambda = i\omega$, so that $\operatorname{Re}\lambda = 0$. In this case, (20) amounts to

$$(21) \quad z_3^*(W + W^T)z_3 + z_4^*(G + G^T)z_4 = 0.$$

The reader can easily check that if P is positive definite, then $v^*(P + P^T)v$ is real and positive for any nonvanishing possibly complex vector v . Hence, from (21) we get $z_3 = z_4 = 0$, making (16) amount to

$$(22a) \quad B_c z_1 + \lambda B_l L z_2 + B_i z_5 = 0,$$

$$(22b) \quad \lambda Q_c C z_1 + Q_l z_2 + Q_v z_6 = 0.$$

The absence of ICL-cutsets makes $\mathcal{Q}_{ICL} = \ker(B_c \ B_l \ B_i) = \{0\}$ (in the light of (7)), and because of the nonvanishing and nonsingularity assumptions on λ and L , the identity (22a) yields $z_1 = z_2 = z_5 = 0$. In turn, (22b) leads to $z_6 = 0$ because V-loops are precluded, so that $\ker Q_v = 0$. This would imply that all entries in the corresponding eigenvector do vanish, showing that the absence of ICL-cutsets rules out (nonzero) purely imaginary eigenvalues. The reader can proceed analogously in order to show that the same happens if there are no VCL-loops. \square

Remark 1. If the eigenvalue analysis is restricted to the pencil (15), the assumption that the circuit has neither VC-loops nor IL-cutsets can be removed. Indeed, if in Proposition 2 we assume that the circuit may display these configurations, the proof proceeds by showing that (22a) implies $z_1 = 0$, but then (22b) yields $z_2 = z_6 = 0$, and the absence of I-cutsets in well-posed circuits leads to $z_5 = 0$. Similarly, the corank analysis in Proposition 1 does not make use of the absence of VC-loops and IL-cutsets. This requirement just drives the analysis to an index one setting; VC-loops or IL-cutsets would make the DAE (1) index two, and the reduction would be somewhat more involved than (3). Cf. in this regard Example 2 in section 5.

Our main result, stated in Theorem 1 below, is an immediate consequence of Propositions 1 and 2.

THEOREM 1. *Consider an equilibrium point of a memristive circuit. Suppose that, at equilibrium, the memductance and conductance matrices W, G are positive definite, and the capacitance and inductance matrices C, L are symmetric and nonsingular. Assume also that at least one of the following two sets of topological conditions holds:*

- *the circuit does not have VC-loops, VL-loops, or ICL-cutsets; or*
- *it does not have IL-cutsets, IC-cutsets, or VCL-loops.*

Then, locally around the equilibrium the state-space dimension of the circuit dynamics is defined by the number of memristors and reactive elements, and there is a manifold of equilibria whose dimension is given by the number of memristors and which is normally hyperbolic.

Proof. Note that ICL-cutsets preclude in particular IL- and IC-cutsets, whereas VCL-loops rule out VC- and VL-loops. Hence, the claim about the state-space dimension is just a consequence of the fact that in this setting the matrix $g_y(x^*, y^*)$ in

(8) is nonsingular and, therefore, the dynamics is locally modelled by an explicit ODE (of the form (3)) formulated in terms of v_c, i_l, φ_m . The existence of a normally hyperbolic manifold of equilibria whose dimension is given by the number of memristors follows directly from the equilibrium conditions (5) and Propositions 1 and 2. \square

THEOREM 2. *Under the assumptions of Theorem 1, the manifold of equilibria attracts all nearby trajectories if, additionally, the capacitance and inductance matrices C, L are positive definite.*

Proof. This claim follows from the Šoštaišvili–Palmer theorem (cf. [3, 30]) once we note that the real part of all the remaining eigenvalues is known to be nonzero, and that the assumption $\operatorname{Re}\lambda > 0$ would lead to $z_1 = z_2 = z_3 = z_4 = 0$ in (20) and then $z_5 = z_6 = 0$ in (22); this would yield $z = 0$ as the unique solution of (16). \square

4. Bifurcation without parameters. Let us now assume that the topological conditions stated in Theorems 1 and 2 are met, but that some variable reaches a value in which the positive definiteness assumption on a circuit matrix (e.g., on the memductance W) fails. The existence of a manifold of equilibria itself is not affected, since as indicated before it relies only on the fact that the memristors' fluxes φ_m do not enter the equilibrium conditions (5). However, the assumptions supporting the normal hyperbolicity and the exponential stability of this manifold no longer hold, and a bifurcation without parameters might be displayed.

4.1. Explicit ODEs. Broadly speaking, such a bifurcation may occur in one of two ways. First, even under the failure of the definiteness assumption on some circuit matrix it may happen that the matrix g_y in (8) is nonsingular. The reduction (3) still applies in this setting, and the analysis can be driven to the context of explicit ODEs $x' = F(x)$. In particular, *lines* of equilibria are often addressed splitting $x = (u, v)$ and $F = (F_1, F_2)$ to write

$$(23a) \quad u' = F_1(u, v),$$

$$(23b) \quad v' = F_2(u, v),$$

with $u \in \mathbb{R}^{n-1}$, $v \in \mathbb{R}$, $F(0, v) = 0$ (cf. [15, 16, 17]; see also [2, 18, 25]). The qualitative properties of equilibria $(0, v)$ may change as v increases through 0; for instance, a *transcritical* bifurcation without parameters may follow from a real loss of stability when an additional eigenvalue of the linearization crosses zero; a Hopf bifurcation may result from a complex loss of stability, that is, from the crossing of a pair of eigenvalues through the imaginary axis.

In this framework, it is important to distinguish cases in which the bifurcation can be reduced to a “classical” setting, namely, problems in which there exists a foliation by invariant sets transverse to the line of equilibria. In these cases, one can reduce (23b) to $v' = 0$ (possibly after a change of coordinates), and v becomes a parameter. Certain nondegeneracy conditions on (23) avoid this. For example, in the transcritical bifurcation, in which F_{1_u} undergoes a simple zero eigenvalue at the origin, the condition $F_{2_u}(0, 0)w \neq 0$ for $w \in \ker F_{1_u} - \{0\}$ rules out such a foliation and therefore avoids the reduction to classical bifurcation theory. Instances of a transcritical bifurcation without parameters and a Hopf bifurcation (which can be reduced to a classical setting) will be discussed in section 5.

4.2. Bifurcation without parameters in DAEs. Things are different if the failing of the positive definite assumption referred to above makes the nonsingularity of the matrix g_y break down. Now the explicit reduction (3) is no longer feasible, and new dynamic phenomena, arising specifically from the differential-algebraic form of

the system, may be expected. In particular, one eigenvalue of the linearization (which is described by a matrix pencil) may diverge through $\pm\infty$, resulting in the loss of the exponential stability of the equilibrium manifold; Theorem 3 below addresses this phenomenon along a line of equilibria. This behavior is reminiscent of the eigenvalue divergence phenomenon analyzed in the context of parametrized DAEs in [5, 36, 38, 46, 47] and references therein. This phenomenon is often termed a *singularity-induced bifurcation* (SIB), because it arises when, along an equilibrium branch, the matrix g_y becomes singular at a given parameter value; this results in a change in the local qualitative properties of the flow. The reader is referred to [5, 38, 46] for details about this phenomenon in parametrized DAEs.

In Theorem 3 we do not restrict our attention to the semistate models arising in circuit analysis, but consider general semiexplicit DAEs instead, since the result is believed to be of independent interest in this broader setting. Conditions which preclude certain foliations, reducing the problem to a scenario with classical parameters, will be discussed in subsection 5.4.

THEOREM 3. *Consider a semiexplicit DAE,*

$$(24a) \quad x' = f(x, y),$$

$$(24b) \quad 0 = g(x, y),$$

with $f \in C^1(\mathbb{R}^n, \mathbb{R}^r)$, $g \in C^1(\mathbb{R}^n, \mathbb{R}^p)$, $n = r + p$, and let the following assumptions hold:

1. The DAE has a C^1 -curve of equilibria through a given (x^*, y^*) .

2. $\text{rk} \begin{pmatrix} f_x & f_y \\ g_x & g_y \end{pmatrix} = n$ at (x^*, y^*) .

3. The pencil $\lambda \begin{pmatrix} I & 0 \\ 0 & 0 \end{pmatrix} - \begin{pmatrix} f_x & f_y \\ g_x & g_y \end{pmatrix}$ has Kronecker index two at (x^*, y^*) .

Then, the local flow defined by the DAE is r -dimensional around equilibrium points $(x, y) \neq (x^*, y^*)$; one eigenvalue of the linearization vanishes identically, and another one diverges through $\pm\infty$ as the equilibrium curve undergoes the point (x^*, y^*) . If the remaining $r - 2$ eigenvalues lie on the left half-plane, this divergence results in the loss of exponential stability of the curve of equilibria.

Proof. The rank condition stated in item 2 implies that

$$\text{rk} \begin{pmatrix} f_x & f_y \\ g_x & g_y \end{pmatrix} = n - 1$$

at (x^*, y^*) . This means that there exist $n - 1$ components of (f, g) (to be grouped together into a map F) and $n - 1$ variables out of $x_1, \dots, x_r, y_1, \dots, y_p$ (to be denoted by u ; write the remaining variable as v) for which the derivative \tilde{F}_u is locally nonsingular; here we are denoting the permutation of variables as $(x, y) = \zeta(u, v)$ and $\tilde{F}(u, v) = F(\zeta(u, v))$.

Note that the asserted existence of a curve of equilibrium implies that the remaining component of $f_1, \dots, f_r, g_1, \dots, g_p$ locally vanishes when F does so. We may then apply the implicit function theorem to describe the curve of equilibria as $u = h(v)$ for some locally defined map h with $h'(v) = -(\tilde{F}_u(h(v), v))^{-1} \tilde{F}_v(h(v), v)$. Set, additionally, $(u^*, v^*) = \zeta^{-1}(x^*, y^*)$ and $\delta(u, v) = \det g_y(\zeta(u, v))$.

The rank condition stated in item 2 can be recast as

$$(25) \quad \text{rk} \begin{pmatrix} \tilde{F}_u & \tilde{F}_v \\ \delta_u & \delta_v \end{pmatrix} = n$$

at (u^*, v^*) . But the Schur complement of \tilde{F}_u in this matrix is

$$-\delta_u \tilde{F}_u^{-1} \tilde{F}_v + \delta_v,$$

which, evaluated at $(h(v), v)$, is nothing but the derivative of $\det g_y$ along the equilibrium curve, that is,

$$(26) \quad \frac{d\delta(h(v), v)}{dv}.$$

Hence, the maximal rank statement expressed by (25) means that the derivative (26) does not vanish at v^* . This implies that $\det g_y(\zeta(h(v), v))$ is not zero in a neighborhood of v^* , except at the point v^* itself (note that the Kronecker index two condition in item 3 implies in particular that $\det g_y(\zeta(h(v), v))$ vanishes at v^*); in turn, this means that the dynamics is r -dimensional around equilibria $\zeta(h(v), v) \neq (x^*, y^*)$.

The linearization along the equilibrium curve $\zeta(h(v), v)$ then leads to the study of the spectrum of a one-parameter matrix pencil,

$$(27) \quad \lambda \begin{pmatrix} I & 0 \\ 0 & 0 \end{pmatrix} - \begin{pmatrix} H_{11}(v) & H_{12}(v) \\ H_{21}(v) & H_{22}(v) \end{pmatrix},$$

as in [5, 36]. In (27), $H_{11}(v)$ stands for the partial derivatives f_x evaluated at $\zeta(h(v), v)$, etc. We have $\det H_{22}(v) = \det g_y(\zeta(h(v), v)) = \delta(h(v), v)$, and the remarks above show that

$$\det H_{22}(v^*) = 0, \quad (\det H_{22})'(v^*) \neq 0.$$

For later use, notice that the second condition implies $\text{rk } H_{22}(v^*) = p - 1$. Note also that the Kronecker index of the pencil (27) is one for v sufficiently close (but not equal) to v^* , since $\det H_{22}(v) \neq 0$ for these v , and two at v^* . Additionally, the existence of the curve of equilibria automatically means that one eigenvalue of (27) vanishes identically.

The index one nature of the pencil in a punctured neighborhood of v^* implies that the determinant of (27) reads as

$$(28) \quad a_r(v)\lambda^r + a_{r-1}(v)\lambda^{r-1} + \dots + a_1(v)\lambda,$$

with $a_0(v) = 0$ because of the vanishing of one eigenvalue. Elementary matrix properties yield $a_r(v) = \det(-H_{22}(v))$, so that $a_r(v^*) = 0$, $a'_r(v^*) \neq 0$.

By applying the differentiation index notion [7] to the pencil (27), the fact that the Kronecker index of the pencil is two at v^* implies that the index of

$$(29) \quad \lambda \begin{pmatrix} I & 0 \\ -H_{21}(v^*) & -H_{22}(v^*) \end{pmatrix} - \begin{pmatrix} H_{11}(v^*) & H_{12}(v^*) \\ 0 & 0 \end{pmatrix}$$

is one. The number of eigenvalues in the (finite) spectrum of this pencil is then given by the rank of the leading matrix, which equals $r + p - 1$ because $\text{rk } H_{22}(v^*) = p - 1$. But, again, elementary properties of determinants show that the determinant of (29) equals that of (27) (at v^*) except for a λ^p factor. This means that (28) has $r - 1$ roots for $v = v^*$, so that $a_{r-1}(v^*) \neq 0$.

Altogether, the conditions $a_r(v^*) = 0$, $a'_r(v^*) \neq 0$, $a_{r-1}(v^*) \neq 0$ imply that one root of (28) diverges through $\pm\infty$ as v undergoes the value v^* (see, e.g., [47]); equivalently, one pencil eigenvalue diverges as (x, y) takes on the value (x^*, y^*) along the equilibrium curve, as claimed. Finally, the loss of exponential stability when the diverging eigenvalue jumps to the positive semiaxis, provided that the remaining ones lie on the left half-plane, is straightforward. \square

Instances of this bifurcation can be found in Examples 1 and 3 below.

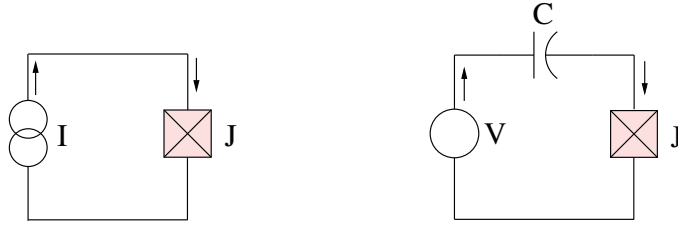


FIG. 1. (a) Phase and (b) charge qubits based on the Josephson junction.

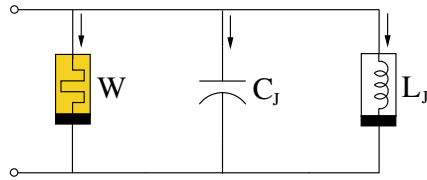


FIG. 2. Equivalent model of the Josephson junction accommodating memristive effects.

5. Examples.

5.1. Superconducting qubits. Much research has been focused on quantum computation in recent decades (see, e.g., [10, 29, 32] and references therein). A key issue in this field is the implementation of a *quantum bit* or *qubit*, that is, a two-level quantum system which can be controlled and read out [10, 11, 29, 32, 48]. Qubit designs are often based on the Josephson tunneling junction, which consists of two superconducting films separated by an insulating layer. There are several alternatives for the implementation of such a superconducting quantum bit; among others, these include the *phase qubit*, defined by a current-biased Josephson junction in which the qubit states are defined by quantized energy levels, and the *charge qubit*, based on a Cooper pair box [10, 11, 48]; cf. Figure 1.

The main feature of the Josephson junction is a nonlinear current-flux relation of the form $i_l = I_0 \sin(k_0 \varphi_l)$ for certain positive constants I_0, k_0 . From this point of view, the device behaves as a nonlinear inductor, with inverse incremental inductance $L_J^{-1}(\varphi_l) = I_0 k_0 \cos(k_0 \varphi_l)$. However, as detailed in [9, 23], realistic models of the Josephson junction should also take into account the presence of capacitive, resistive, and memristive effects. Figure 2 displays an equivalent circuit for the junction which includes a flux-controlled memristor (accommodating both resistive and memristive effects), a linear capacitor and a nonlinear inductor. As reported in [9, 23], the flux-controlled memristor captures the presence of a small current component given by $i_m = Gv + I_1 \cos(k_1 \varphi_m)v$ for certain constants G, I_1, k_1 ; note that the term Gv accounts for a linear resistive effect. The memductance reads as $W(\varphi_m) = G + I_1 \cos(k_1 \varphi_m)$. The linear capacitor has positive capacitance C_J .

In the following subsections we examine the role of the memristor in the dynamics of the circuits displayed in Figure 1.

5.2. Example 1: The phase qubit. Using the model of Figure 2 for the Josephson junction, we arrive at the equivalent circuit displayed in Figure 3 for the

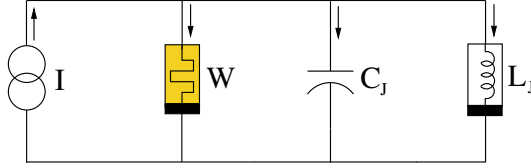


FIG. 3. Equivalent circuit of a phase qubit.

phase qubit. The dynamics of this circuit is easily seen to be defined by the model

$$(30a) \quad \varphi'_m = v,$$

$$(30b) \quad \varphi'_l = v,$$

$$(30c) \quad C_J v' = I - W(\varphi_m)v - I_0 \sin(k_0 \varphi_l).$$

Throughout the whole discussion it will be assumed that $|I| < I_0$. Equilibria are defined by the conditions $v = 0$, $\sin(k_0 \varphi_l) = I/I_0$, and those for which $\cos(k_0 \varphi_l)$ is positive exhibit a positive incremental inductance L_J .

Let us first neglect the memristive currents, that is, assume $G = I_1 = 0$ in the memristor characteristic, so that $W(\varphi_m)$ vanishes identically. This corresponds to open-circuiting the memristor in Figure 3, and results in an ICL-cutset and an LC-loop, which are in turn responsible for a pair of purely imaginary eigenvalues in the linearization about equilibria with $L_J > 0$. Indeed, disregarding (30a) and the term $W(\varphi_m)v$ in (30c), an easy computation yields the eigenvalues $\lambda = \pm i \sqrt{(L_J C_J)^{-1}}$.

The ICL-cutset is broken, however, when the memristor is taken into account. Now the variable φ_m actually enters the model but not the equilibrium conditions; this means that the circuit has a one-dimensional manifold of equilibria. Assuming that $W > 0$, in the light of Theorems 1 and 2 this manifold should be normally hyperbolic provided that $L_J \neq 0$ and exponentially stable in cases with $L_J > 0$. Simple computations show that there is indeed a null eigenvalue and a pair

$$(31) \quad \lambda = \frac{-W}{2C_J} \pm \sqrt{\left(\frac{W}{2C_J}\right)^2 - \frac{1}{L_J C_J}}.$$

Fixing $W > 0$, $C_J > 0$, the real parts of these eigenvalues are nonnull if $L_J \neq 0$, and actually negative if $L_J > 0$.

Note that the memductance W depends on the flux φ_m . If φ_m undergoes a value in which $W(\varphi_m)$ becomes negative, there is a stability change along the manifold of equilibrium. As $W(\varphi_m)$ vanishes, the eigenvalues (31) cross the imaginary axis through a purely imaginary conjugate pair, leading generically to a Hopf bifurcation. The exponential stability of the equilibrium manifold is lost as a consequence of the fact that the memristor becomes locally active.

Another case of interest arises from neglecting the capacitive effect within the Josephson junction. Making $C_J = 0$ (that is, removing the capacitor from Figure 3), the dynamics becomes two-dimensional and is described by the DAE

$$(32a) \quad \varphi'_m = v,$$

$$(32b) \quad \varphi'_l = v,$$

$$(32c) \quad 0 = I - W(\varphi_m)v - I_0 \sin(k_0 \varphi_l).$$

Consistent with Theorems 1 and 2, one eigenvalue vanishes, whereas the other one equals $\lambda = -(L_J W)^{-1}$, being negative if $L_J > 0$ and $W > 0$.

Now, when the flux φ_m reaches a value φ_m^* such that $W(\varphi_m^*) = 0$, provided that $W'(\varphi_m^*) \neq 0$ this eigenvalue diverges through $\pm\infty$, the manifold of equilibria becoming unstable for negative values of $W(\varphi_m)$. This is a consequence of Theorem 3. Indeed, the model (32) has the semiexplicit form depicted in (24). The curve of equilibrium points is defined by $v = 0$, $\sin(k_0\varphi_l) = I/I_0$, being parametrized by the memristor flux φ_m . Up to a sign change, the determinant $\det g_y$ in Theorem 3 amounts in this case to W , and the equilibrium becomes singular when W vanishes. Because of the assumption $W'(\varphi_m^*) \neq 0$, the transversality condition in item 2 of Theorem 3 does hold. Additionally, at singular equilibria the pencil arising in item 3 can be checked to be index two. This shows that the bifurcation can be understood to be a consequence of Theorem 3.

5.3. Example 2: The charge qubit. Our second example illustrates that the eigenvalue analysis of section 3 is also valid in the presence of topologically degenerate configurations, namely, VC-loops and/or IL-cutsets (cf. Remark 1 in section 3.3). With this aim, consider the equivalent circuit displayed in Figure 4 for the charge qubit, based again on the Josephson junction model of Figure 2.

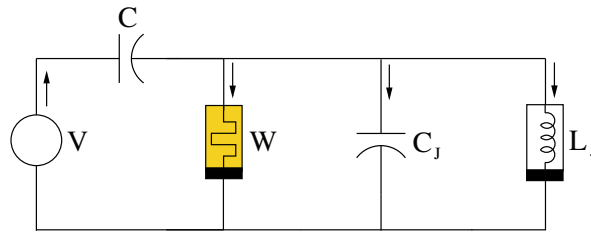


FIG. 4. Equivalent circuit of a charge qubit.

The circuit includes three reactive elements and a memristor, which altogether introduce four dynamic variables. However, the presence of a VC-loop defined by the voltage source V , the gate capacitor C (the voltage across it to be denoted below by v_c), and the Josephson capacitor C_J (with voltage v) restricts the possible values of v_c and v , making the actual state-space three-dimensional.

The circuit equations read as

$$\begin{aligned}
 (33a) \quad & \varphi_m' = v, \\
 (33b) \quad & \varphi_l' = v, \\
 (33c) \quad & C v_c' = i_{c_J} + W(\varphi_m)v + I_0 \sin(k_0\varphi_l), \\
 (33d) \quad & C_J v' = i_{c_J}, \\
 (33e) \quad & 0 = v_c + v - V,
 \end{aligned}$$

where (33e) captures the constraint among the branch voltages imposed by the VC-loop. Equilibrium points are given by $v = i_{c_J} = 0$, $\sin(k_0\varphi_l) = 0$, $v_c = V$, with no restriction on φ_m ; this means that there is a one-dimensional manifold of equilibria, as expected. The spectrum is easily checked to be defined by the pair of eigenvalues

$$\lambda = \frac{-W}{2(C + C_J)} \pm \sqrt{\left(\frac{W}{2(C + C_J)}\right)^2 - \frac{1}{L_J(C + C_J)}},$$

in addition to a null one. Again, the nonvanishing eigenvalues have a non-zero real part if $W > 0$ and C, C_J, L_J are not null, and these real parts are actually negative if C, C_J, L_J are positive. In the former case, the manifold of equilibria is normally hyperbolic, becoming exponentially stable in the latter.

As in Example 1, values of φ_m for which $W(\varphi_m)$ vanishes yield generically a Hopf bifurcation: indeed, provided that C, C_J, L_J are positive, the pair of nonvanishing eigenvalues crosses the imaginary axis towards the right half-plane as W becomes negative. This can be seen as an unfolding of the case in which memristive effects are ignored, since, if we disregard the presence of the memristor (that is, if we make $G = I_1 = 0$ in the memristor characteristic, so that W vanishes identically), we arrive at a pair of purely imaginary eigenvalues $\lambda = \pm i\sqrt{(L_J(C + C_J))^{-1}}$. This purely imaginary pair now follows from the presence of a VCL-loop and an LC-cutset.

5.4. Foliation by invariant hyperplanes. Examples 1 and 2 above exhibit a family of hyperplanes which are invariant for the dynamics, namely, $\varphi_m - \varphi_l = k \in \mathbb{R}$. To fix ideas, consider the system (30); from (30a) and (30b) it is clear that $\varphi'_m - \varphi'_l = 0$, and therefore $\varphi_m - \varphi_l$ is a conserved quantity for the flow. Moreover, the hyperplanes $\varphi_m - \varphi_l = k$ are transversal to the equilibrium lines. Via a linear change of coordinates, we may then define $\mu = \varphi_m - \varphi_l$ as a parameter (since $\mu' = 0$), and the bifurcation phenomena can be addressed in the setting of “classical” bifurcation theory. For instance, fixing the circuit parameters $C_J = I_0 = k_0 = I_1 = k_1 = 1, G = 1/2, I = 0$, a supercritical Hopf bifurcation is displayed by (30) at the origin when the parameter μ undergoes the value $\mu^* = 2\pi/3$.

In both examples, this reduction to a classical setting is a consequence of the presence of a loop defined by the memristor and the nonlinear inductor; indeed, this yields the identity $v_m = v_l$ between the voltage drops in both devices; that is, $\varphi'_m = \varphi'_l$. The linearity of this restriction is due to the linear nature of Kirchhoff laws; it is important to provide circuit-theoretic conditions ruling out in general the existence of such linear foliations and the corresponding reduction to classical bifurcation theory. Note that, for specific types of bifurcations, it is possible to provide nondegeneracy conditions precluding such a reduction under possibly nonlinear coordinate changes (cf. the transcritical bifurcation without parameters discussed in Example 4).

Consider in this regard the explicit ODE (23). A foliation by hyperplanes transversal to the line of equilibria would be defined by an invariant of the form $v - L(u)$, L being a linear function. By differentiating w.r.t. time, we would get a linear relation between the components of the vector field F , namely $F_2(u, v) = L(F_1(u, v))$, making the Jacobian matrix $F'(u, v)$ everywhere singular. This means that a nonsingularity requirement on the Jacobian matrix F' (away from the equilibrium line) precludes the existence of the aforementioned foliations by hyperplanes.

Such a nonsingularity requirement can be evaluated in circuit-theoretic terms. For the sake of simplicity consider a circuit with only one memristor, so that the equilibrium manifold is a line. The matrix of derivatives of the right-hand side of (1) at an arbitrary point reads as

$$\begin{pmatrix} 0 & 0 & 0 & I_c & 0 & 0 & 0 & 0 & 0 & 0 & 0 \\ 0 & 0 & 0 & 0 & I_l & 0 & 0 & 0 & 0 & 0 & 0 \\ 0 & 0 & 0 & 0 & 0 & I_m & 0 & 0 & 0 & 0 & 0 \\ 0 & 0 & W'(\varphi_m)v_m & 0 & 0 & -W(\varphi_m) & 1 & 0 & 0 & 0 & 0 \\ 0 & 0 & 0 & 0 & 0 & 0 & 0 & -G(v_r) & I_r & 0 & 0 \\ B_c & 0 & 0 & 0 & B_l & B_m & 0 & B_r & 0 & B_i & 0 \\ 0 & Q_l & 0 & Q_c & 0 & 0 & Q_m & 0 & Q_r & 0 & Q_v \end{pmatrix}.$$

Assuming that $W'(\varphi_m) \neq 0$ (at least near equilibrium), at points with $v_m \neq 0$ the nonsingularity of this matrix is easily checked to be equivalent to that of

$$\begin{pmatrix} B_c & 0 & 0 & B_r & B_i & 0 \\ 0 & Q_l & Q_m & Q_r G & 0 & Q_v \end{pmatrix},$$

and as an easy application of Lemma 1 this nonsingularity requirement amounts to the absence of IC-cutsets and VML-loops. This means that in circuits with positive definite conductance and a single flux-controlled memristor verifying $W'(\varphi_m) \neq 0$ at equilibrium, the absence of IC-cutsets and VML-loops rules out the existence of foliations by hyperplanes transversal to the equilibrium line. Note that the ML-loop of Examples 1 and 2 is a particular case of a VML-loop.

5.5. Example 3: SIB without parameters. As detailed above, the existence of a “classical” bifurcation parameter $\varphi_m - \varphi_l$ in Examples 1 and 2 follows from the existence of an ML-loop. By breaking such a loop, we get a simple example of the aforementioned phenomenon of eigenvalue divergence without such a foliation by hyperplanes.

A series connection of a flux-controlled memristor with memductance $W(\varphi_m)$, a linear inductor with positive inductance L , and a linear resistor with positive resistance R (cf. Figure 5(a)) is easily seen to be governed by the DAE

$$\begin{aligned} \varphi_m' &= v_m, \\ Li_l' &= -Ri_l - v_m, \\ 0 &= i_l - W(\varphi_m)v_m. \end{aligned}$$

Equilibria are defined by $i_l = v_m = 0$. Provided that for a given φ_m^* we have $W(\varphi_m^*) = 0$, $W'(\varphi_m^*) \neq 0$, the hypotheses of Theorem 3 may be checked to hold. Along the equilibrium line the nonvanishing eigenvalue reads as $\lambda = -(WR + 1)(WL)^{-1}$, and, as expected, it diverges through $\pm\infty$ as φ_m undergoes the critical value φ_m^* .

Note that in this case there is no linear foliation if $R \neq 0$; in contrast, if we make $R = 0$ (that is, by short-circuiting the resistor, so that the circuit displays an ML-loop), we would get the linear invariant $\varphi_m + Li_l$, akin to Examples 1 and 2.

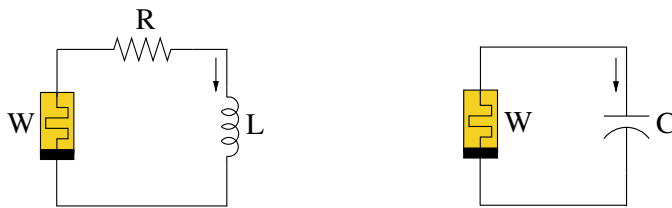


FIG. 5. *Bifurcation without parameters in nonlinear circuits: (a) SIB, (b) transcritical bifurcation.*

5.6. Example 4: A transcritical bifurcation without parameters. Finally, a series connection of a flux-controlled memristor and a linear capacitor (Figure 5(b)) yields a simple instance of a transcritical bifurcation without parameters (cf. [15, 18, 25] and references therein). Letting v be the voltage drop at the memristor, the circuit equations are

$$\begin{aligned} Cv' &= -W(\varphi_m)v, \\ \varphi_m' &= v. \end{aligned}$$

Equilibria are given by $v = 0$, and the conditions $W(\varphi_m^*) = 0$, $W'(\varphi_m^*) \neq 0$ at a given φ_m^* yield a double zero eigenvalue (with geometric multiplicity one) at φ^* ; provided that the capacitance C is positive, the equilibrium line loses stability as W becomes negative.

Consistent with the analysis in the references [15, 18, 25] mentioned above, the nondegeneracy condition $W'(\varphi_m^*) \neq 0$ rules out in this example the existence of any kind of foliation transversal to the equilibrium line and hence the reduction to a classical bifurcation framework. The characterization in circuit-theoretic terms of these and other features of transcritical bifurcations without parameters in general memristive circuits is an open problem.

As a final remark, it is worth noting that by choosing $C = 1$, $W(\varphi_m) = -\varphi_m$ and writing $v \equiv x$, $\varphi_m \equiv y$, the equations of this circuit are made to take exactly the normal form

$$\begin{aligned}x' &= xy, \\y' &= x,\end{aligned}$$

derived in [15].

6. Concluding remarks. Some analytical properties of manifolds of equilibria arising in memristive circuits have been explored in this paper. We have provided graph-theoretic conditions which guarantee the normal hyperbolicity of such manifolds, as well as their exponential stability under additional passivity requirements. The failing of certain passivity assumptions along the manifold of equilibria has motivated the analysis of bifurcations without parameters in general semiexplicit DAEs. Our results apply to certain circuits arising in the design of quantum bits based on the Josephson tunneling junction, accurate models of which incorporate memristive effects.

Several lines of research remain open. The full characterization of normally hyperbolic configurations in memristive circuits requires further study in cases without strict passivity assumptions. Bifurcations without parameters in DAEs and, specifically, in memristive circuit models can be analyzed in broader generality. Finally, the results might be extended to circuits including memcapacitors and meminductors (cf. [12]), and also to distributed circuit models involving partial differential-algebraic equations (PDAEs).

Acknowledgment. The author gratefully acknowledges several remarks from an anonymous reviewer regarding the theory of bifurcation without parameters and Examples 1 and 2.

REFERENCES

- [1] S. ADEE, *Memristor inside*, IEEE Spectrum, Sept. 2010; online at <http://spectrum.ieee.org/semiconductors/devices/memristor-inside>.
- [2] A. AFENDIKOV, B. FIEDLER, AND S. LIEBSCHER, *Plane Kolmogorov flows and Takens-Bogdanov bifurcation without parameters: The doubly reversible case*, Asymptot. Anal., 60 (2008), pp. 185–211.
- [3] B. AULBACH, *Continuous and Discrete Dynamics near Manifolds of Equilibria*, Lecture Notes in Math. 1058, Springer, New York, 1984.
- [4] B. BAO, Z. MA, J. XU, Z. LIU, AND Q. XU, *A simple memristor chaotic circuit with complex dynamics*, Internat. J. Bifur. Chaos Appl. Sci. Engrg., 21 (2011), pp. 2629–2645.
- [5] R. E. BEARDMORE, *The singularity-induced bifurcation and its Kronecker normal form*, SIAM J. Matrix Anal. Appl., 23 (2001), pp. 126–137.

- [6] B. BOLLOBÁS, *Modern Graph Theory*, Springer-Verlag, New York, Berlin, 1998.
- [7] K. E. BRENNAN, S. L. CAMPBELL, AND L. R. PETZOLD, *Numerical Solution of Initial-Value Problems in Differential-Algebraic Equations*, Classics in Appl. Math. 14, SIAM, Philadelphia, 1995.
- [8] L. O. CHUA, *Memristor—The missing circuit element*, IEEE Trans. Circuit Theory, 18 (1971), pp. 507–519.
- [9] L. O. CHUA, *Nonlinear circuit foundations for nanodevices, Part I: The four-element torus*, Proc. IEEE, 91 (2004), pp. 1830–1859.
- [10] J. CLARKE AND F. K. WILHELM, *Superconducting quantum bits*, Nature, 453 (2008), pp. 1031–1042.
- [11] M. H. DEVORET, A. WALLRAFF, AND J. M. MARTINIS, *Superconducting Qubits: A Short Review*, preprint, 2004, available online at <http://arxiv.org/abs/cond-mat/0411174>.
- [12] M. DI VENTRA, Y. V. PERSHIN, AND L. O. CHUA, *Circuit elements with memory: Memristors, memcapacitors and meminductors*, Proc. IEEE, 97 (2009), pp. 1717–1724.
- [13] R. DIESTEL, *Graph Theory*, Springer-Verlag, New York, Berlin, 2000.
- [14] D. ESTÉVEZ-SCHWARZ AND C. TISCHENDORF, *Structural analysis of electric circuits and consequences for MNA*, Intl. J. Circuit Theory Appl., 28 (2000), pp. 131–162.
- [15] B. FIEDLER, S. LIEBSCHER, AND J. C. ALEXANDER, *Generic Hopf bifurcation from lines of equilibria without parameters: I. Theory*, J. Differential Equations, 167 (2000), pp. 16–35.
- [16] B. FIEDLER AND S. LIEBSCHER, *Generic Hopf bifurcation from lines of equilibria without parameters: II. Systems of viscous hyperbolic balance laws*, SIAM J. Math. Anal., 31 (2000), pp. 1396–1404.
- [17] B. FIEDLER, S. LIEBSCHER, AND J. C. ALEXANDER, *Generic Hopf bifurcation from lines of equilibria without parameters: III. Binary oscillations*, Internat. J. Bifur. Chaos Appl. Sci. Engrg., 10 (2000), pp. 1613–1622.
- [18] B. FIEDLER AND S. LIEBSCHER, *Takens-Bogdanov bifurcations without parameters and oscillatory shock profiles*, in Global Analysis of Dynamical Systems, H. W. Broer, B. Krauskopf, and G. Vegter, eds., Institute of Physics, Bristol, UK, 2001, pp. 211–259.
- [19] M. GÜNTHER AND U. FELDMANN, *CAD-based electric-circuit modeling in industry. I: Mathematical structure and index of network equations*, Surveys Math. Indust., 8 (1999), pp. 97–129.
- [20] R. A. HORN AND CH. R. JOHNSON, *Matrix Analysis*, Cambridge University Press, Cambridge, UK, 1985.
- [21] M. ITOH AND L. O. CHUA, *Memristor oscillators*, Internat. J. Bifur. Chaos Appl. Sci. Engrg., 18 (2008), pp. 3183–3206.
- [22] M. ITOH AND L. O. CHUA, *Memristor Hamiltonian circuits*, Internat. J. Bifur. Chaos Appl. Sci. Engrg., 21 (2011), pp. 2395–2425.
- [23] D. JELTSEMA AND A. J. VAN DER SCHAFT, *Memristive port-Hamiltonian systems*, Math. Comp. Model. Dyn. Sys., 16 (2010), pp. 75–93.
- [24] O. KAVEHEI, A. IQBAL, Y. S. KIM, K. ESHRAGHIAN, S. F. AL-SARAWI, AND D. ABBOTT, *The fourth element: Characteristics, modelling and electromagnetic theory of the memristor*, Proc. R. Soc. A, 466 (2010), pp. 2175–2202.
- [25] S. LIEBSCHER, *Dynamics near manifolds of equilibria of codimension one and bifurcation without parameters*, Electron. J. Differential Equations, 63 (2011), 112.
- [26] M. MESSIAS, C. NESPOLI, AND V. A. BOTTA, *Hopf bifurcation from lines of equilibria without parameters in memristors oscillators*, Internat. J. Bifur. Chaos Appl. Sci. Engrg., 20 (2010), pp. 437–450.
- [27] B. MUTHUSWAMY, *Implementing memristor-based chaotic circuits*, Internat. J. Bifur. Chaos Appl. Sci. Engrg., 20 (2010), pp. 1335–1350.
- [28] B. MUTHUSWAMY AND L. O. CHUA, *Simplest chaotic circuit*, Internat. J. Bifur. Chaos Appl. Sci. Engrg., 20 (2010), pp. 1567–1580.
- [29] M. A. NIELSEN AND I. L. CHUANG, *Quantum Computation and Quantum Information*, Cambridge University Press, Cambridge, UK, 2000.
- [30] K. J. PALMER, *Linearization near an integral manifold*, J. Math. Anal. Appl., 51 (1975), pp. 243–255.
- [31] Y. V. PERSHIN AND M. DI VENTRA, *Practical approach to programmable analog circuits with memristors*, IEEE Trans. Circuits Systems I, 57 (2010), pp. 1857–1864.
- [32] Y. V. PERSHIN AND M. DI VENTRA, *Neuromorphic, digital, and quantum computation with memory circuit elements*, Proc. IEEE, 100 (2012), pp. 2071–2080.
- [33] Y. V. PERSHIN AND M. DI VENTRA, *Memory effects in complex materials and nanoscale systems*, Adv. Phys., 60 (2011), pp. 145–227.

- [34] P. J. RABIER AND W. C. RHEINBOLDT, *Theoretical and numerical analysis of differential-algebraic equations*, in Handbook of Numerical Analysis VIII, North-Holland, Amsterdam, 2002, pp. 183–540.
- [35] T. REIS, *Circuit synthesis of passive descriptor systems—A modified nodal approach*, Int. J. Circuit Theory Appl., 38 (2010), pp. 44–68.
- [36] R. RIAZA, *On the singularity-induced bifurcation theorem*, IEEE Trans. Automat. Control, 47 (2002), pp. 1520–1523.
- [37] R. RIAZA, *Differential-Algebraic Systems. Analytical Aspects and Circuit Applications*, World Scientific, River Edge, NJ, 2008.
- [38] R. RIAZA, *Stability loss in quasilinear DAEs by divergence of a pencil eigenvalue*, SIAM J. Math. Anal., 41 (2010), pp. 2226–2245.
- [39] R. RIAZA, *Explicit ODE reduction of memristive systems*, Internat. J. Bifur. Chaos Appl. Sci. Engrg., 21 (2011), pp. 917–930.
- [40] R. RIAZA AND C. TISCHENDORF, *Qualitative features of matrix pencils and DAEs arising in circuit dynamics*, Dyn. Syst., 22 (2007), pp. 107–131.
- [41] R. RIAZA AND C. TISCHENDORF, *The hyperbolicity problem in electrical circuit theory*, Math. Methods Appl. Sci., 33 (2010), pp. 2037–2049.
- [42] R. RIAZA AND C. TISCHENDORF, *Semistate models of electrical circuits including memristors*, Int. J. Circuit Theory Appl., 39 (2011), pp. 607–627.
- [43] D. B. STRUKOV, G. S. SNIDER, D. R. STEWART, AND R. S. WILLIAMS, *The missing memristor found*, Nature, 453 (2008), pp. 80–83.
- [44] M. TAKAMATSU AND S. IWATA, *Index characterization of differential-algebraic equations in hybrid analysis for circuit simulation*, Int. J. Circuit Theory Appl., 38 (2010), pp. 419–440.
- [45] C. TISCHENDORF, *Topological index calculation of DAEs in circuit simulation*, Surveys Math. Indust., 8 (1999), pp. 187–199.
- [46] V. VENKATASUBRAMANIAN, H. SCHÄTTLER, AND J. ZABORSZKY, *Local bifurcations and feasibility regions in differential-algebraic systems*, IEEE Trans. Automat. Control, 40 (1995), pp. 1992–2013.
- [47] L. YANG AND Y. TANG, *An improved version of the singularity-induced bifurcation theorem*, IEEE Trans. Automat. Control, 46 (2001), pp. 1483–1486.
- [48] A. ZAGOSKIN AND A. BLAIS, *Superconducting qubits*, La Physique au Canada, 63 (2007), pp. 215–227.